Check for updates

PNPase and RhlB Interact and Reduce the Cellular Availability of Oxidized RNA in *Deinococcus radiodurans*

Runhua Han,[a] Jessie Jiang,[a] Jaden Fang,[a] Lydia M. Contreras[a,b]

[a]McKetta Department of Chemical Engineering, The University of Texas at Austin, Austin, Texas, USA
[b]Institute for Cellular and Molecular Biology, The University of Texas at Austin, Austin, Texas, USA

ABSTRACT 8-Oxo-7,8-dihydroguanine (8-oxoG) is a major RNA modification caused by oxidative stresses and has been implicated in carcinogenesis, neurodegeneration, and aging. Several RNA-binding proteins have been shown to have a binding preference for 8-oxoG-modified RNA in eukaryotes and protect cells from oxidative stress. To date, polynucleotide phosphorylase (PNPase) is one of the most well-characterized proteins in bacteria that recognize 8-oxoG-modified RNA, but how PNPase cooperates with other proteins to process oxidized RNA is still unclear. Here, we use RNA affinity chromatography and mass spectrometry to search for proteins that preferably bind 8-oxoG-modified RNA in *Deinococcus radiodurans*, an extremophilic bacterium with extraordinary resistance to oxidative stresses. We identified four proteins that preferably bind to oxidized RNA: PNPase (DR_2063), DEAD box RNA helicase (DR_0335/RhlB), ribosomal protein S1 (DR_1983/RpsA), and transcription termination factor (DR_1338/Rho). Among these proteins, PNPase and RhlB exhibit high-affinity binding to 8-oxoG-modified RNA in a dose-independent manner. Deletions of PNPase and RhlB caused increased sensitivity of *D. radiodurans* to oxidative stress. We further showed that PNPase and RhlB specifically reduce the cellular availability of 8-oxoG-modified RNA but have no effect on oxidized DNA. Importantly, PNPase directly interacts with RhlB in *D. radiodurans*; however, no additional phenotypic effect was observed for the double deletion of *pnp* and *rhlB* compared to the single deletions. Overall, our findings suggest the roles of PNPase and RhlB in targeting 8-oxoG-modified RNAs and thereby constitute an important component of *D. radiodurans* resistance to oxidative stress.

IMPORTANCE Oxidative RNA damage can be caused by oxidative stress, such as hydrogen peroxide, ionizing radiation, and antibiotic treatment. 8-oxo-7,8-dihydroguanine (8-oxoG), a major type of oxidized RNA, is highly mutagenic and participates in a variety of disease occurrences and development. Although several proteins have been identified to recognize 8-oxoG-modified RNA, the knowledge of how RNA oxidative damage is controlled largely remains unclear, especially in nonmodel organisms. In this study, we identified four RNA binding proteins that show higher binding affinity to 8-oxoG-modified RNA compared to unmodified RNA in the extremophilic bacterium *Deinococcus radiodurans*, which can endure high levels of oxidative stress. Two of the proteins, polynucleotide phosphorylase (PNPase) and DEAD-box RNA helicase (RhlB), interact with each other and reduce the cellular availability of 8-oxoG-modified RNA under oxidative stress. As such, this work contributes to our understanding of how RNA oxidation is influenced by RNA binding proteins in bacteria.

KEYWORDS 8-oxo-7, 8-dihydroguanine, *Deinococcus radiodurans*, PNPase, RNA binding proteins, RNA oxidation, RhlB, oxidative stress

Reactive oxygen species (ROS) are generated either through basal cellular metabolism or from external environmental exposures to oxidative stresses, such as ionizing radiation, UV radiation, air pollution, and certain chemicals (1, 2). Importantly, increased

levels of ROS can attack and damage various important cellular components, especially nucleic acids (3, 4). Both DNA and RNA oxidation are closely related to a variety of pathophysiological events, including carcinogenesis, aging, and chronic neurodegenerative diseases (5–9). In particular, compared to DNA, RNAs are more susceptible to oxidative insults given the relatively higher cellular abundance of RNA and their single-stranded nature that lacks protection offered by hydrogen bonding and specific proteins (10). Thus far, mechanisms affecting the cellular accumulation of RNA oxidation have been less characterized relative to DNA oxidation.

Among the known oxidative lesions in RNA, 7,8-dihydro-8-oxoguanosine (8-oxoG) is one of the most prevalent nucleobase oxidations (9, 11). 8-oxoG modifications on RNA can extensively interfere with translation, as well as with the base pairing of RNAs, including that of noncoding RNAs (12–14). To avoid the detrimental effects of 8-oxoG, organisms are equipped with mechanisms that eliminate oxidized RNA (15–17). As an example, the MutT protein in *Escherichia coli* and its mammalian homologs (such as MutT homolog 1 [MTH1]) cleave ribonucleotides carrying 8-oxoG by hydrolyzing the oxidized nucleoside diphosphates and/or triphosphates to monophosphates (18, 19), preventing the incorporation of the free oxidized nucleotides into RNA synthesis. Although the oxidized forms of RNA precursor nucleotides can be efficiently removed in such manner, 8-oxoG can also be formed in the RNA molecules already present within the cell by direct oxidation of the base (20). Unlike DNA oxidation, no dedicated repair mechanism for RNA oxidation has been identified thus far; it has been considered that oxidatively damaged RNAs are only degraded rather than repaired (21). Importantly, several RNA-binding proteins (RBPs) have been reported to preferentially bind RNAs containing 8-oxoG and contribute to the fidelity of translation in cells by eliminating the oxidized RNA away from the translational machinery (8, 15, 17, 22, 23). In mammalian cells, for example, the Auf1 protein (AU-rich element RNA-binding protein 1) preferably binds to RNA carrying one 8-oxoG residue to eliminate oxidatively damaged mRNA (24), whereas poly(C)-binding proteins PCBP1 and PCBP2 bind to more severely oxidized RNAs containing at least two 8-oxoG residues and induce the activation of apoptotic reactions (25, 26).

Relative to mammalian cells, understanding the interaction between RBPs and 8-oxoG in bacteria still lags behind. Polynucleotide phosphorylase (PNPase), a conserved 3′-5′ exoribonuclease, is the only characterized RBP that interacts with 8-oxoG-modified RNA in bacteria (27). Both *E. coli* PNPase and human PNPase have been shown to bind 8-oxoG-modified RNA with higher affinity than to unmodified RNA (28, 29). The preferential binding of PNPase to RNAs containing 8-oxoG suggests a role in RNA quality control; indeed, PNPase has been shown to reduce the accumulation of RNAs containing 8-oxoG and to protect cells under oxidative stress (27, 30, 31). Interestingly, PNPase can form multiprotein complexes in many bacteria (32–34). In *E. coli*, PNPase functions as part of the RNA degradosome complex that also contains the endoribonuclease RNase E, a DEAD-box RNA helicase RhlB, and the glycolytic enzyme enolase Eno (33). The interaction of RNase E, PNPase, and RhlB can ensure their functional cooperation and is required for an efficient RNA degradation (33). For instance, RhlB is known to unwind RNA structures in *E. coli* and therefore facilitates degradation by PNPase (35, 36). PNPase and RhlB can also form a complex independent of the degradosome and therefore can be involved in alternative protein-protein interactions (37). However, whether RhlB cooperates with PNPase to affect oxidized RNA under oxidative stress is still unknown.

Deinococcus radiodurans is a unique bacterium that possesses remarkable tolerance to extreme environmental conditions that generate oxidative damage to macromolecules (38). The survival and recovery capabilities of *D. radiodurans* postexposure to those extreme environmental stresses is remarkable, particularly considering that it undergoes high levels of RNA oxidation under some of these oxidative stresses. As an example, a significant increase of 8-oxoG-modified RNA has been observed under 15 kGy of ionizing radiation (39). However, little is known as to how oxidated RNA is managed in this organism. The 8-oxoG-recognizing protein, PNPase, is present in *D. radiodurans* and contributes to

the survival under hydrogen peroxide (H_2O_2) and UV radiation (40). Interestingly, *D. radiodurans* also encodes many other DEAD box RNA helicases (e.g., RhlB, DR_B0136/HepA, and DR_1624) (41). However, whether and how they modulate 8-oxoG-modified RNAs in *D. radiodurans* is still unclear.

Here, through a combination of RNA affinity chromatography, mass spectrometry and biochemical analysis, we demonstrate that PNPase and RhlB in *D. radiodurans* exhibit high-affinity binding to 8-oxoG modified RNA relative to unmodified RNA in a dose-independent manner. The deletion of PNPase and RhlB significantly impairs the survival of *D. radiodurans* under H_2O_2 stress and results in elevated levels of 8-oxoG-modified RNA (not 8-oxoG-modified DNA). Most importantly, PNPase interacts with RhlB, and no additive effect on survival and 8-oxoG-RNA level was observed in the double-deletion strain of PNPase and RhlB relative to the single-deletion strains. The latter result suggests that PNPase and RhlB may function cooperatively to defend against oxidative stress in *D. radiodurans*. To the best of our knowledge, this is the first study that indicates the essential role of RBPs in response to cellular damage induced by oxidative stresses in *D. radiodurans*.

RESULTS

Potential 8-oxoG-binding RBPs in *D. radiodurans* are identified via RNA affinity chromatography. To identify RBPs that preferably bind to 8-oxoG-modified RNA in *D. radiodurans*, we conducted an RNA affinity chromatography approach followed by liquid chromatography-tandem mass spectrometry (LC-MS/MS) analysis (Fig. 1A). Two types of 24-mer synthetic RNA oligonucleotides were used: a bait oligonucleotide carrying an 8-oxoG modification and a control oligonucleotide carrying unmodified guanines. After incubating with cell lysates extracted from the *D. radiodurans* R1 strain, different proteins were pulled down using the 8-oxoG-modified and control RNA oligonucleotides, as revealed by SDS-PAGE electrophoresis and principal-component analysis (see Fig. S1A and B in the supplemental material).

Both sets of proteins eluted from the pulldown experiments were then subjected to LC-MS/MS. A total of 111 proteins were significantly enriched (log_2 fold change $\geq$ 0.58496, $P \leq 0.05$) in the pulldown from the 8-oxoG-modified oligonucleotide relative to the control oligonucleotide (Fig. 1B; see also Table S1). Gene ontology and enrichment analysis showed that the proteins enriched in the pulldown using the 8-oxoG-modified oligonucleotide are involved in a variety of pathways, including DNA replication, nucleic acid phosphodiester bond hydrolysis, cellular component organization or biogenesis, and nucleotide excision repair (Fig. 1C). We also revealed a complex protein-protein interacting network among these proteins through the STRING-DB database (42) (see Fig. S1C). We suspect that the tightly connected protein-protein interaction network partially explains the high number of proteins that were identified from these assays. Notably, many proteins involved in RNA degradation and in RNA binding and nuclease activity were enriched in the 8-oxoG pulldown (see Table S1), suggesting the possibility that the interactions of these proteins with 8-oxoG-modified RNA could lead to its degradation. We further identified 10 RBPs that contain known RNA-binding domains (Fig. 1B; see also Table S1), including DR_2063/PNPase (the PNPase homolog in *D. radiodurans*), DR_0335/RhlB (DEAD box RNA helicase), DR_1983/RpsA (ribosomal protein S1), DR_1338/Rho (Rho transcription termination factor), DR_0353/Rnr (RNase R), DR_1797/NusA (transcription elongation factor NusA), DR_1836/Ffh (signal recognition particle protein), and other three ribosomal proteins (RplM, RpsH, and RpsB). These results suggest that these proteins could possibly directly bind to 8-oxoG-modified RNA. Interestingly, DR_0550/MutT was also found to be enriched in the 8-oxoG pulldown (see Table S1). Considering that DR_0550/MutT does not contain any known RNA-binding domain and can only recognize the oxidized RNA precursor nucleotides, not the RNA molecules oxidized after transcription (19), we believe that this might be from indirect protein-protein interaction or unspecific binding. As such, we excluded this protein from further analysis.
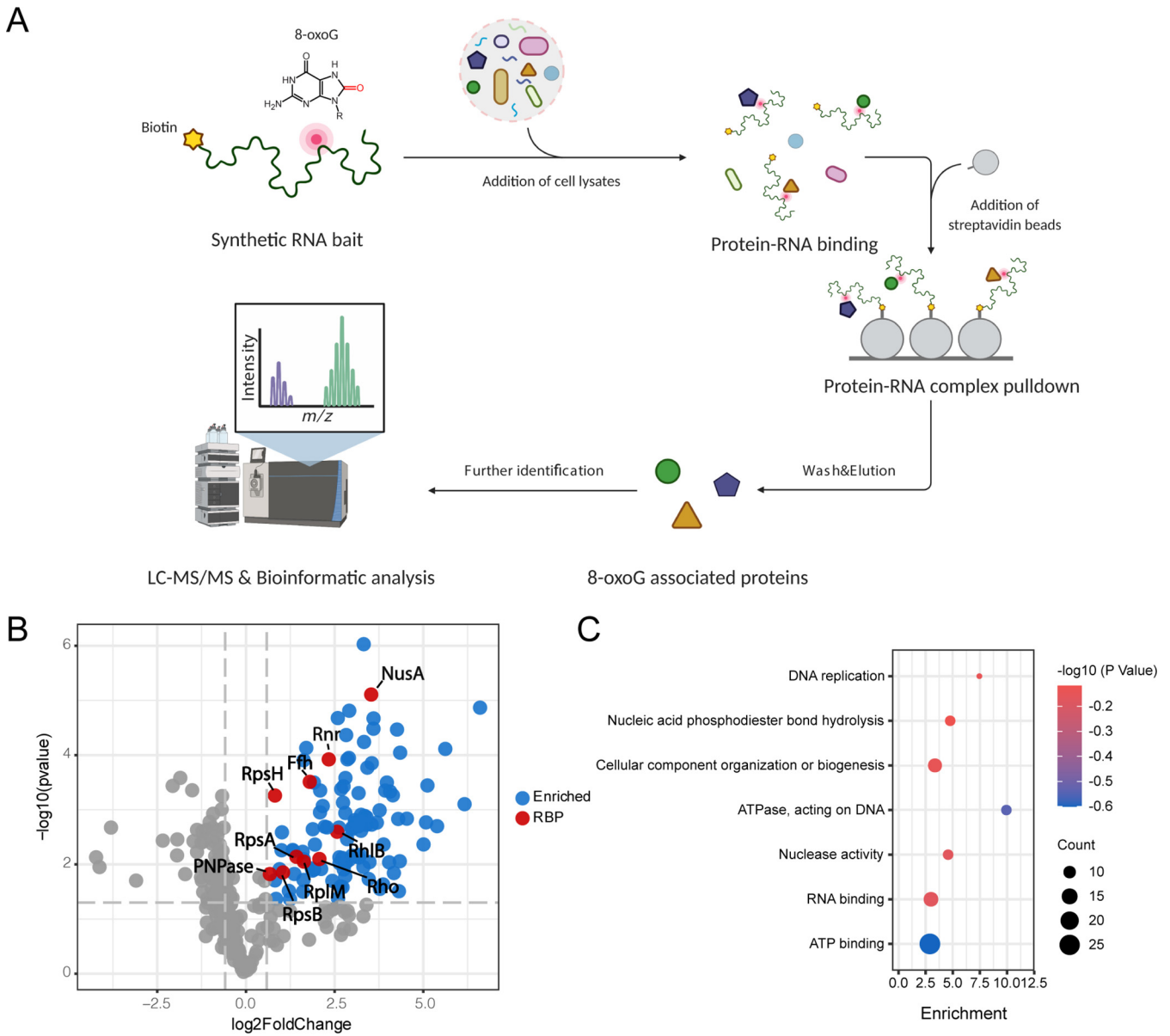
FIG 1 RNA affinity chromatography identifies putative 8-oxoG binding proteins in *D. radiodurans*. (A) The RNA affinity chromatography approach using biotinylated RNA oligonucleotides containing one 8-oxoG modification followed by LC-MS/MS and downstream analysis was used to identify novel 8-oxoG binding proteins in *D. radiodurans*. (B) A volcano plot shows the enrichment of proteins bound to the 8-oxoG-modified oligonucleotide versus the unmodified control oligonucleotide. Proteins that are significantly enriched (log$_2$ fold change $\geq$ 0.58496, $P \leq 0.05$) are highlighted by blue (for those without known RNA-binding domains) or red (for those containing known RNA-binding domains) (listed in Table S1). Proteins that are not significantly enriched are represented by gray dots. (C) Gene ontology and enrichment analysis of the proteins significantly enriched in RNA affinity chromatography.

PNPase, RhlB, Rho, and RpsA preferably bind to 8-oxoG oxidized RNA in *D. radiodurans*. To further confirm that the enrichment of these RBPs in the 8-oxoG pull-down assay reflected their preference for binding 8-oxoG-modified RNA, we purified proteins of PNPase, RhlB, RpsA, Rho, NusA, Rnr, and Ffh (RplM, RpsH, and RpsB were excluded from the further analysis given their roles in rRNA binding). Each purified protein was incubated with oligoribonucleotides carrying one 8-oxoG or no 8-oxoG; these mixtures were subjected to RNA affinity chromatography, and pulldown products were subjected to Western blotting. As shown in Fig. 2A and B, PNPase, RhlB, Rho, and RpsA exhibited selective binding to the oligoribonucleotide containing 8-oxoG compared to the control oligoribonucleotide. In contrast, Rnr and NusA showed similar binding to both oligoribonucleotides, and no Ffh protein was detected in the pulldown fractions
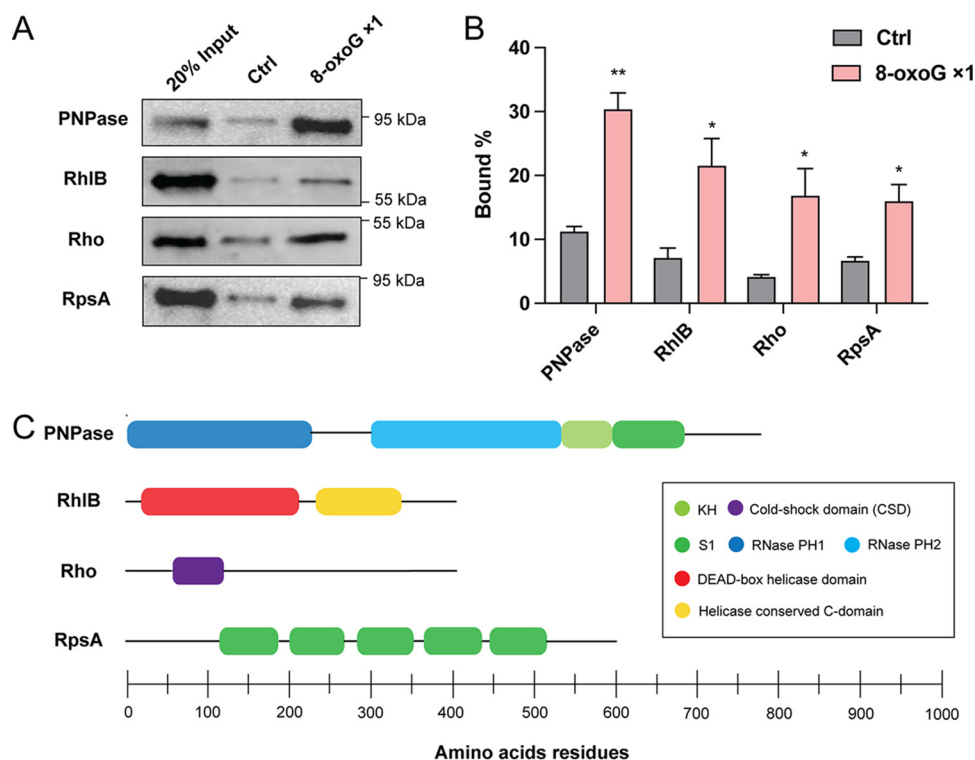
FIG 2 RBPs preferably bind 8-oxoG-modified oligoribonucleotide in *D. radiodurans*. (A) Binding of PNPase, RhlB, Rho, and RpsA to oligoribonucleotides carrying one 8-oxoG (8-oxoG ×1) and control oligoribonucleotide (Ctrl), as determined by Western blotting. 500 ng of each purified recombinant protein was incubated with 10 μg of biotinylated oligoribonucleotide carrying one 8-oxoG or no 8-oxoG and then subjected to 500 μg of Dynabead MyOne Streptavidin C1 beads. After incubation, the beads were washed, and the proteins were resuspended in SDS sample buffer. Western blotting was performed to detect the proteins in the input and the pulldown fractions with an anti-His$_6$ antibody. In addition, 20% input: 20% of each recombinant protein applied to binding was also subjected to Western blotting. (B) The band intensities were measured by CLIQS (TotalLab), and the percentage bound was determined. Error bars represent the standard deviations of biological triplicates. Significance was calculated by two-tailed Student *t* test compared to Ctrl under each condition (*, $P \leq 0.05$; **, $P \leq 0.01$). (C) Domain composition of PNPase, RhlB, Rho, and RpsA. RNA-binding domains are represented as rounded boxes and color coded as indicated in the box.

from either oligoribonucleotide (see Fig. S2). These results indicated that, among these proteins, only PNPase, RhlB, Rho, and RpsA selectively bound 8-oxoG-modified RNA, whereas the enrichment of Ffh, Rnr, and NusA in the RNA affinity chromatography is likely from indirect protein-protein interactions (i.e., from interactions with PNPase, RhlB, Rho, or RpsA). It is worth noting that all of these proteins contain known RNA-binding domains that play diverse roles in RNA metabolisms, such as KH and S1 (43–45) (Fig. 2C), suggesting that these domains might be important for 8-oxoG recognition in *D. radiodurans*.

We next attempted to quantify the binding affinity of the PNPase, RhlB, Rho, and RpsA to 8-oxoG-modified RNAs using electrophoretic mobility shift assays (EMSAs). In these assays, the same RNA oligoribonucleotides used in the affinity chromatography assay were radiolabeled and incubated with purified PNPase, RhlB, RpsA, and Rho at different concentrations, followed by electrophoresis in native PAGE gels. As shown in Fig. S3 in the supplemental material, all four proteins exhibited higher binding affinity to the 8-oxoG-containing oligoribonucleotide than the control oligoribonucleotide. Importantly, quantification of the dissociation constant (K_d) showed that PNPase and RhlB bind to 8-oxoG-modified oligoribonucleotide with high affinity at the nanomolar range (30.0 $\pm$ 1.4 nM and 382.9 $\pm$ 47.4 nM, respectively) (Fig. 3A and B; Table 1). In contrast, RpsA and Rho showed relatively lower affinity to the 8-oxoG-modified oligoribonucleotides (1,705.1 $\pm$ 305.7 nM and 1,882.3 $\pm$ 21.2 nM) (Fig. 3C and D; Table 1).
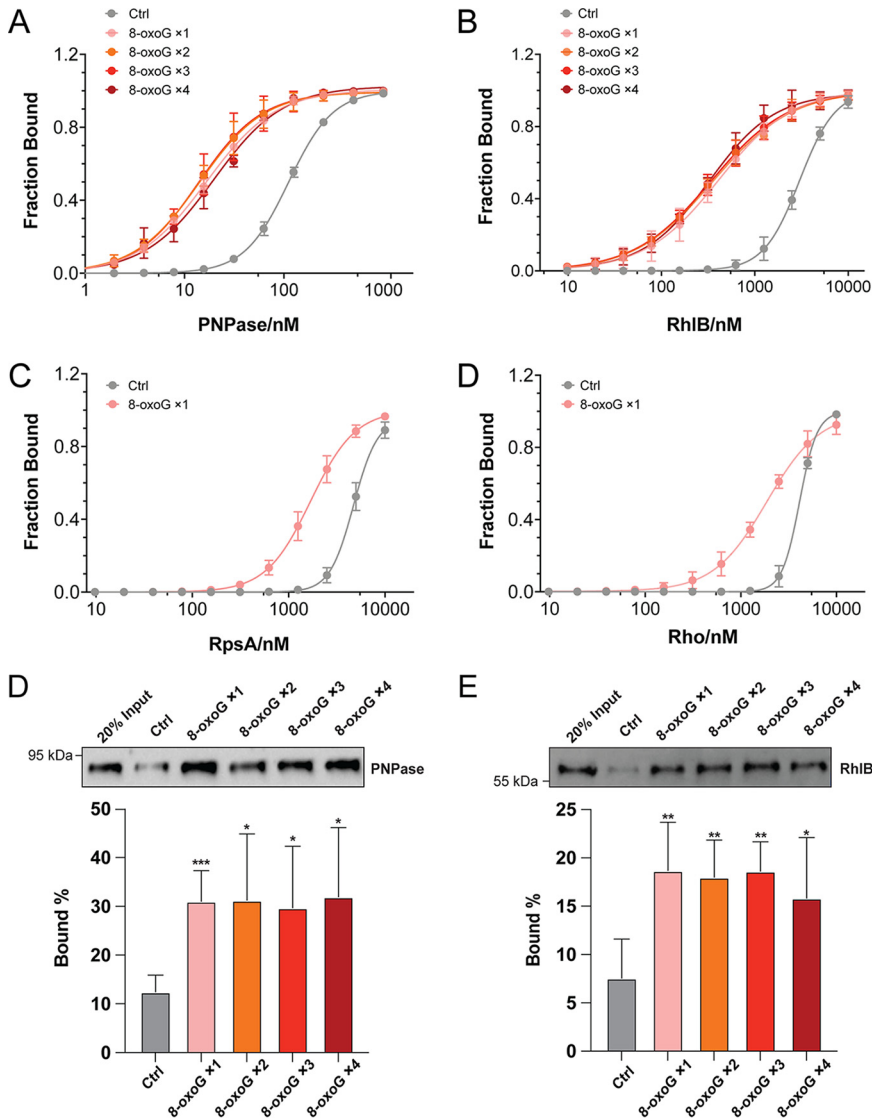
FIG 3 Determination of binding capability of 8-oxoG recognizing RBPs to 8-oxoG-modified and unmodified oligonucleotides. Binding affinities of PNPase (A), RhlB (B), Rho (C), and RpsA (D) to oligonucleotides carrying different numbers of 8-oxoG bases (8-oxoG ×1-4) and control oligonucleotide (Ctrl) were determined by EMSA. The dissociation constant (K_d) values were measured in duplicates and are summarized in Table 1. The binding of PNPase and RhlB to oligoribonucleotides carrying 8-oxoG bases and control oligoribonucleotide was also evaluated by RNA affinity chromatography, followed by Western blotting (for PNPase [E] and RhlB [F], respectively). The band intensities shown in the bottom panels were measured by CLIQS (TotalLab), and the percentage bound was determined. Data from five independent experiments are shown. Significance was calculated by using a two-tailed Student t test compared to Ctrl under each condition (*, $P \leq 0.05$; **, $P \leq 0.01$; ***, $P \leq 0.001$).

These results suggest that, among the four proteins, PNPase and RhlB are prominent RBPs that recognize 8-oxoG-modified RNA in *D. radiodurans*. We therefore selected these proteins for further study.

The binding of PNPase and RhlB to 8-oxoG-modified RNA is dose independent. Previous studies indicate that certain RBPs may have the ability to differentiate mildly from heavily oxidized RNA in HeLa cells (25, 26). To explore whether PNPase and RhlB have a similar function, we repeated the EMSA analysis using synthetic oligoribonucleotides containing one to four 8-oxoG bases. As shown in Fig. 3A and B and Table 1, both PNPase and RhlB showed an equivalent binding affinity to the oligoribonucleotides carrying different numbers of 8-oxoGs, which is significantly higher than the binding to the control oligonucleotide without 8-oxoG. We further confirmed this result

TABLE 1 Binding affinities of 8-oxoG-recognizing RBPs for 8-oxoG-modified oligonucleotides and unmodified control oligonucleotide[a]

		Mean K_d (nM) $\pm$ the SD				
Protein ID	Name	Ctrl	8-oxoG ×1	8-oxoG ×2	8-oxoG ×3	8-oxoG ×4
DR_2063	PNPase	111.6 $\pm$ 7.2	30.0 $\pm$ 1.4	28.9 $\pm$ 4.2	29.4 $\pm$ 8.7	24.7 $\pm$ 1.4
DR_0335	RhlB	3,005.2 $\pm$ 137.0	382.9 $\pm$ 47.4	354.8 $\pm$ 56.7	351.2 $\pm$ 80.8	340.6 $\pm$ 47.1
DR_1983	RpsA	5,444.1 $\pm$ 403.6	1,705.1 $\pm$ 305.7	ND	ND	ND
DR_1338	Rho	3,942.2 $\pm$ 286.1	1,882.3 $\pm$ 21.2	ND	ND	ND

[a]Dissociation constants (K_d) and standard deviations were determined in duplicate by electrophoretic mobility shift assays (Fig. 3; see also Fig. S3). 8-oxoG×1 to 8-oxoG×4, 8-oxoG-modified oligonucleotides; Ctrl, unmodified control oligonucleotide; ND, not determined.

through RNA affinity chromatography assay followed by Western blotting: we found that the binding capacity of PNPase and RhlB to oligonucleotides carrying different numbers of 8-oxoGs is similar, which is significantly higher relative to the binding with the control oligonucleotide (Fig. 3E and F). These results indicate that the binding pocket of PNPase and RhlB can be saturated by only one 8-oxoG, which prevents the further binding of additional 8-oxoG bases.

PNPase and RhlB are essential to the survival of *D. radiodurans* under H_2O_2 stress. To further test the biological significance of PNPase and RhlB in *D. radiodurans*, we attempted to completely abolish the expression of these proteins in *D. radiodurans* using a previously described homologous recombination method (46). Full deletion strains of PNPase and RhlB were successfully constructed and confirmed by both genomic PCR (see Fig. S4A) and reverse transcription-quantitative PCR (RT-qPCR) (see Fig. S4B). The wild-type (WT), Δ*pnp*, and Δ*rhlB* strains were then exposed to 0 to 200 mM H_2O_2, an oxidative reagent widely used in experiments to generate oxidative RNA damage (27). The survival of these strains was assessed by serial diluting and plating. As depicted in Fig. 4A, no significant difference in survival of the WT strain was observed within the 0 to 200 mM H_2O_2 dosage range. In contrast, the Δ*pnp* and Δ*rhlB* strains demonstrated significantly impaired survival under 100 and 200 mM H_2O_2 exposure, while their survival under 0 and 50 mM H_2O_2 was comparable to the WT strain (Fig. 4A). Therefore, we conclude that PNPase and RhlB play crucial roles in protecting *D. radiodurans* cells under oxidative stress.

Importantly, significantly lower levels of PNPase and RhlB expression were detected at both mRNA and protein levels under H_2O_2 stress (Fig. 4B to D). It is worth noting that the absence of PNPase or RhlB does not obviously affect cell growth under the nonoxidative stress condition (see Fig. S4C); these results imply that PNPase and RhlB may be more important under oxidative stress conditions relative to non-oxidative stress conditions in *D. radiodurans*. In addition, deletions of PNPase and RhlB do not affect the intracellular H_2O_2 level (see Fig. S4D), which is contrary to the function of catalase (encoded by *katA*), the main antioxidant protein in *D. radiodurans* that removes H_2O_2 from the cells efficiently under oxidative stress (see Fig. S4D). These results suggest that the reduced cell viability of the Δ*pnp* and Δ*rhlB* strains is not due to deficient bacterial growth or reduced H_2O_2 in the cell culture.

PNPase and RhlB reduce the cellular availability of 8-oxoG in RNA under H_2O_2 stress. Given that both PNPase and RhlB showed preferential binding to 8-oxoG-modified RNA, we hypothesized that they may be involved in processing 8-oxoG-modified RNAs in the cells under oxidative stress. To test this, we determined whether the concentration of 8-oxoG-modified RNA is affected *in vivo* by PNPase or RhlB deletion. The WT, Δ*pnp*, and Δ*rhlB* strains were challenged with 0 and 100 mM H_2O_2 for 30 min, followed by RNA extraction and enzyme-linked immunosorbent assays (ELISAs) using a specific 8-oxoG antibody. As shown in Fig. 5A, significantly higher concentrations of 8-oxoG-modified RNA were detected upon H_2O_2 exposure relative to no treatment in all strains. Notably, the levels of 8-oxoG-modified RNA detected in all three strains in the absence of H_2O_2 exposure were comparable. However, increased levels of 8-oxoG-modified RNA were detected in the Δ*pnp* and Δ*rhlB* strains under H_2O_2 compared to the WT strain (Fig. 5A). Importantly, we
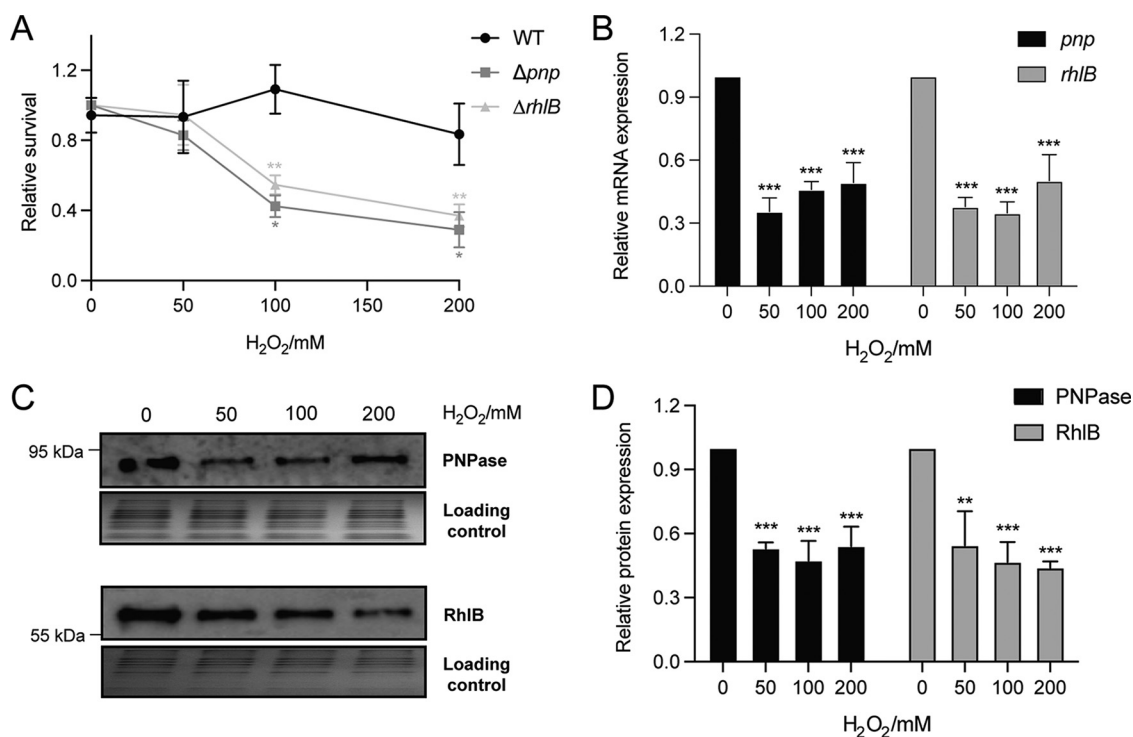
FIG 4 The expression and regulation of PNPase and RhlB are essential for the survival of *D. radiodurans* under H_2O_2. (A) The *D. radiodurans* WT, Δ*pnp*, and Δ*rhlB* strains were grown to the exponential phase and treated with 0, 50, 100, or 200 mM H_2O_2 for 30 min at 4°C. Bacterial survival was evaluated by plate counting after 3 days of incubation at 32°C. The data are represented as the percentages of the untreated control. (B) The mRNA levels of *pnp* and *rhlB* were determined by RT-qPCR. The *D. radiodurans* WT strain was grown to the exponential phase and treated with 0, 50, 100, or 200 mM H_2O_2 for 30 min at 4°C. The total RNA was extracted, and RT-qPCR was carried out to determine the expressions of *pnp* and *rhlB* using gene-specific primers. (C) The protein levels of PNPase and RhlB were determined by Western blotting. The *D. radiodurans* WT strains carrying 3×FLAG chromosomally tagged PNPase and RhlB were grown to the exponential phase and treated with 0, 50, 100, or 200 mM H_2O_2 for 30 min at 4°C. The total cell lysates were extracted, and Western blotting was carried out to determine the expressions of PNPase and RhlB with an anti-FLAG antibody. Protein samples were visualized by Coomassie staining in parallel to show the equivalent protein amount loaded in each lane. (D) The band intensities of Western were measured by CLIQS (TotalLab). Error bars represent the standard deviations of biological triplicates. Significance was calculated by using a two-tailed Student *t* test compared to the WT under each condition (*, $P \leq 0.05$; **, $P \leq 0.01$; ***, $P \leq 0.001$).

confirmed the absence of DNA contamination in the RNA samples (see Fig. S4E), suggesting the 8-oxoG changes detected in the ELISAs were not from the DNA contamination in the samples. These results suggest that the expression of PNPase and RhlB can reduce the cellular availability of 8-oxoG-modified RNA.

Given that DNA can also be severely damaged under oxidative stress (9, 10), we further examined whether PNPase and RhlB can also affect DNA oxidation. Interestingly, we found that the levels of 8-oxoG-modified DNA in the Δ*pnp* and Δ*rhlB* strains are not significantly different compared to the WT strain under both 0 and 100 mM H_2O_2 treatment (Fig. 5B). These results suggest that PNPase and RhlB are only required to modulate the cellular availability of 8-oxoG-modified RNA under oxidative stress but have little effect on DNA oxidation. These results also indicate that the reduced viability of the Δ*pnp* and Δ*rhlB* mutant strains under H_2O_2 may be related to the accumulation of oxidated RNA (more so than to the accumulation of oxidized DNA).

PNPase interacts with RhlB and RpsA in *D. radiodurans*. It is worth noting that PNPase can interact with RhlB and RpsA in *E. coli*, either forming an individual complex or as part of the degradosome (36, 47). However, the contribution of these interactions in *D. radiodurans* to oxidative RNA damage, particularly as part of the oxidative stress response remains to be elucidated. To investigate whether PNPase could interact with other 8-oxoG binding proteins in *D. radiodurans*, we expressed C-terminus His_6-tagged PNPase or RhlB on the pRADgro plasmids as baits and used the WT *D. radiodurans*
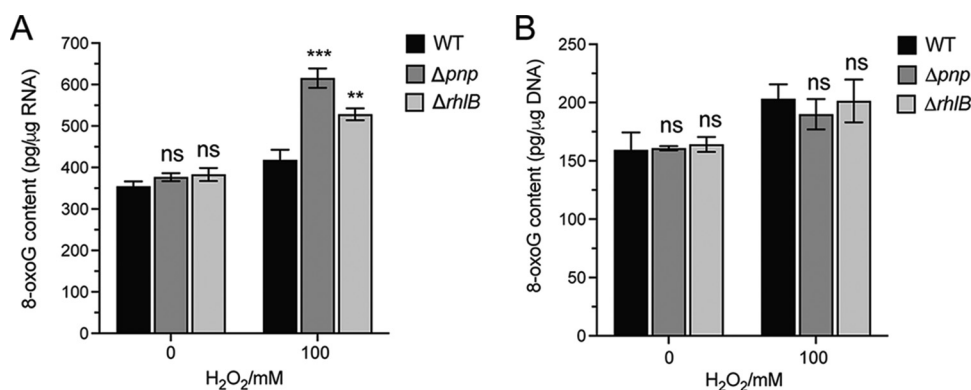
FIG 5 PNPase and RhlB reduce the cellular availability of 8-oxoG-RNA in *D. radiodurans* under H_2O_2. The *D. radiodurans* WT, Δpnp, and $\Delta rhlB$ strains were grown to the exponential phase and treated with 0 or 100 mM H_2O_2 for 30 min at 4°C. Total RNA or DNA was extracted, digested, and subjected to ELISA to determine 8-oxoG-RNA (A) and 8-oxoG-DNA (B) levels.

strain expressing only the His_6 tag on the pRADgro plasmid as the control. We then performed protein-protein coimmunoprecipitation (coIP) experiments, followed by LC-MS/MS analysis, and 584 and 552 proteins were identified in PNPase- and RhlB-coIP experiments, respectively. Among these proteins, 66 proteins were significantly enriched ($\log_2$ fold change ≥ 0.58496, $P \leq 0.05$) in the PNPase-coIP compared to the control strain (Fig. 6A; see also Table S2). In contrast, only 11 proteins were significantly enriched ($\log_2$ fold change ≥ 0.58496, $P \leq 0.05$) in the RhlB-coIP (Fig. 6B; see also Table S2), suggesting the possibility that this protein is involved in a smaller number of protein-protein interactions in *D. radiodurans*. The proteins enriched in the PNPase-coIP include DNA repair proteins (e.g., RecA and Ssb), DNA-directed RNA polymerase subunits (RpoA, RpoB, and RpoC), as well as many ribosomal proteins (see Table S2). Gene ontology and enrichment analysis revealed that these proteins are involved in diverse pathways, especially ribosome assembly/biogenesis, transcription, and translation processes (Fig. 6C). These proteins are also involved in binding to tRNA, mRNA, and rRNA (Fig. 6C). However, it is also possible that (given their abundance) some ribosomal proteins were purified with PNPase due to nonspecific interactions, which has been observed previously (48). Overall, our results from the PNPase-coIP indicate that PNPase participates in large protein-protein networks that likely play important roles in *D. radiodurans*. This is further supported by the STRING-DB analysis showing that 87.88% of these proteins (58 of 66) are potentially interacting with each other (see Fig. S5). Importantly, interactions between 8-oxoG recognizing RBPs were also observed: we identified RhlB and RpsA in the coIP of PNPase (Fig. 6A; see also Table S2) and PNPase in the RhlB-coIP (Fig. 6B; see also Table S2). These data are consistent with the previous studies in *E. coli* (33, 44), and support a model where RhlB or RpsA may form a complex with PNPase to process 8-oxoG-modified RNA in *D. radiodurans*.

We further confirmed the direct interaction of PNPase with RhlB and RpsA in *D. radiodurans* through Western blotting. Protein-protein coIP experiments were performed using the C-terminal His_6-tag PNPase on the pRADgro plasmid as a bait. The anticipated/potential interaction partner (RhlB, RpsA, or Rho) was tagged with 3×FLAG at the C terminus on the chromosome to allow detection by Western blotting with an anti-FLAG antibody. As shown in Fig. 6D, RhlB-3×FLAG and RpsA-3×FLAG were successfully copurified with the strain carrying plasmid expressed His_6-tagged PNPase. Notably, these copurifications were not abolished when cell lysates were treated with RNases, suggesting that the interaction between PNPase with RhlB or RpsA does not rely on their RNA substrates (Fig. 6D). On the contrary, no Rho-3×FLAG was detected in the PNPase-coIP from either RNase-treated or untreated lysates (Fig. 6D). Altogether, our results revealed active interaction between PNPase with RhlB and RpsA in *D. radiodurans* in an RNA-independent manner.
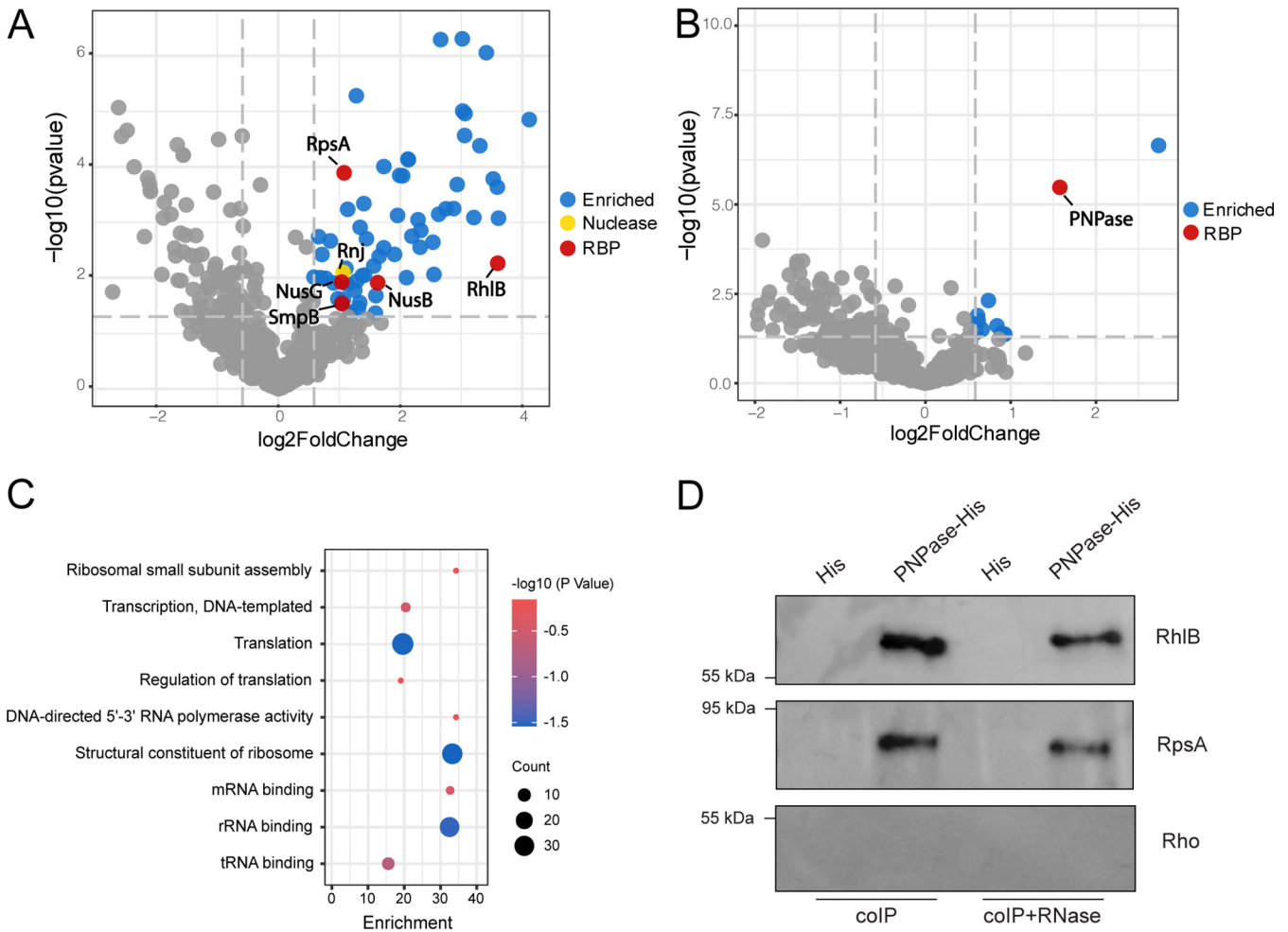
FIG 6 PNPase interacts with RhlB and RpsA in *D. radiodurans*. Volcano plots show the enrichment of proteins in the PNPase-coIP (A) and RhlB-coIP (B). Proteins that are significantly enriched (log$_2$ fold change ≥ 0.58496, $P \leq 0.05$) are highlighted by blue (for those without known RNA-binding domains), red (for those containing known RNA-binding domains), or gold (for those with known nuclease activity) (listed in Table S1). Proteins that are not significantly enriched are represented by gray dots. (C) Gene ontology and enrichment analysis of the proteins significantly enriched in the PNPase-coIP. (D) Confirmation of the interaction of PNPase with RhlB and RpsA. His$_6$ tag or His$_6$-tagged PNPase on pRADgro plasmid was introduced into *D. radiodurans* wild-type strains carrying 3×FLAG chromosomally tagged RhlB, RpsA, or Rho. After cross-linking and sonication, 500-μg of cell lysates were treated with or without RNase A and T1 and then incubated with 50 μL of Ni-NTA magnetic beads. After a washing step, Western blotting was performed to detect the proteins in the pulldown fractions using an anti-FLAG antibody.

RhlB and PNPase double deletion in *D. radiodurans* shows an effect similar to single deletions. Given that PNPase and RhlB show the strongest binding affinity to 8-oxoG-modified RNA among the four 8-oxoG recognizing RBPs (Table 1) and that we were able to confirm their effects on oxidized RNA *in vivo* (Fig. 4 and 5). We further tested whether the association of PNPase with RhlB is important for their functional roles in *D. radiodurans* under oxidative stress. To achieve this, a double deletion strain of *pnp* and *rhlB* (Δ*pnp*Δ*rhlB*) was constructed, and the response of this strain to the H$_2$O$_2$ stress was evaluated. We found that the Δ*pnp*Δ*rhlB* strain exhibited similar survival compared to single-deletion strains (Δ*pnp* and Δ*rhlB*) under H$_2$O$_2$ stress, which is significantly lower than WT under 100 and 200 mM H$_2$O$_2$ (Fig. 7A). In addition, the accumulation of 8-oxoG-RNA in the Δ*pnp*Δ*rhlB* strain was also comparable with that in Δ*pnp* and Δ*rhlB* strains under 100 mM H$_2$O$_2$ (Fig. 7B). These results imply that these two proteins may have redundant activities or function together in modulating RNA oxidation to protect *D. radiodurans* from oxidative stress.

RhlB is an RNA helicase that unfolds structured RNA to promote the degradation of the substrate by PNPase in the *E. coli* (36). To identify the functional role of the PNPase-
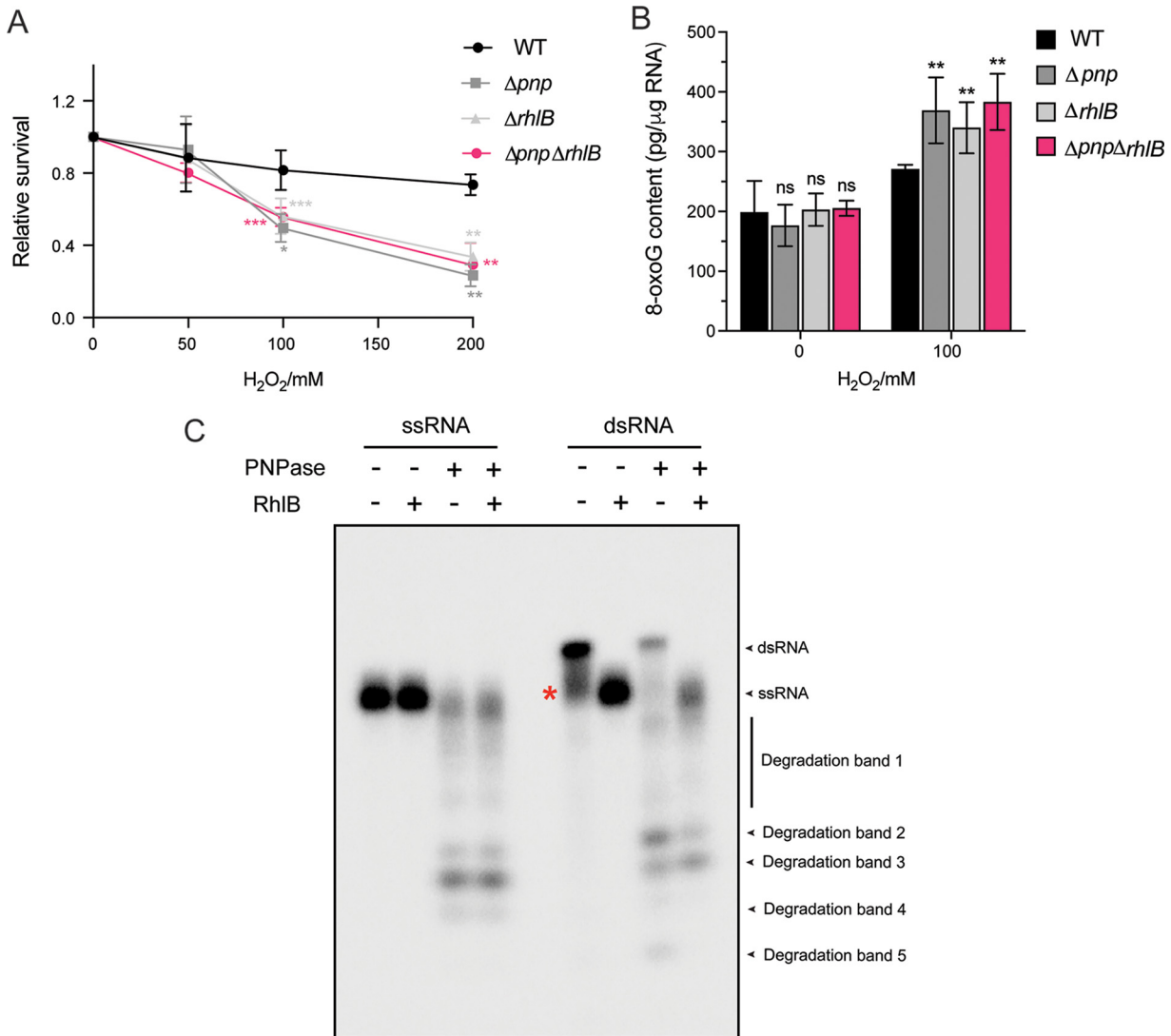
FIG 7 The double-deletion strain of PNPase and RhlB exhibits an effect similar to that for single-deletion strains in *D. radiodurans*. (A) *D. radiodurans* WT, Δ*pnp*, Δ*rhlB*, and Δ*pnp* Δ*rhlB* strains were grown to the exponential phase and treated with 0, 50, 100, or 200 mM H$_2$O$_2$ for 30 min at 4°C. Bacterial survival was evaluated by plate counting after 3 days of incubation at 32°C. The data are represented as percentages of the untreated control. (B) The 8-oxoG-RNA levels in WT, Δ*pnp*, Δ*rhlB*, and Δ*pnp* Δ*rhlB* strains treated with 0 or 100 mM H$_2$O$_2$ were determined by ELISA. Error bars represent the standard deviations of biological triplicates. Significance was calculated by using a two-tailed Student *t* test compared to the WT under each condition (**, $P \leq 0.01$; ***, $P \leq 0.001$). (C) RhlB promotes PNPase degradation on dsRNA in *D. radiodurans*. A synthesized 22-mer ssRNA was radiolabeled at 5′ end and incubated with a short (11-mer) RNA oligonucleotide to form the hybridized dsRNA. RNA degradation and unwinding were evaluated by adding PNPase or RhlB alone or both proteins to ssRNA or dsRNA, followed by 30 min of incubation at 32°C. Reaction products were resolved in a 20% native polyacrylamide gel. The remaining ssRNA residue after hybridization is labeled by a red asterisk. The degradation bands were also labeled.

RhlB interaction in *D. radiodurans*, we examined the degradation of single RNA (ssRNA) and double-stranded RNA (dsRNA) by PNPase *in vitro*. We used a 22-mer ssRNA and an artificial dsRNA as the substrates in PNPase degradation assays in the presence or absence of RhlB. As depicted in Fig. 7C, PNPase can degrade ssRNA, resulting in several bands (degradation bands 1 to 4 in Fig. 7C) but had little effect on dsRNA in the absence of RhlB. However, degradation of the dsRNA reached the same level of ssRNA when RhlB was added to the reaction (Fig. 7C), indicating that the unwinding ability of RhlB can aid the degradation of dsRNA by PNPase in *D. radiodurans*. The partial degradation of the dsRNA when only PNPase was added (degradation bands 1 to 5 in Fig. 7C) may result from the remaining presence of ssRNA (indicated by the red asterisk in Fig. 7C, which we assume is still present in the dsRNA reaction) due to incomplete annealing of the single RNA chain since the hybridization efficiency was not 100%. These results suggest that

PNPase and RhlB may function cooperatively to degrade structured RNA in *D. radiodurans*. It is worth noting that we also attempted to conduct this assay using oligonucleotides carrying 8-oxoG. Unfortunately, no dsRNA can be observed using 8-oxoG-modified oligonucleotides; the presence of 8-oxoG might affect the formation of dsRNA by impairing the base-pairing during RNA-RNA hybridization (14, 49). Further studies are needed to further confirm whether the RhlB can promote the degradation of structured oxidized RNAs.

DISCUSSION

In the past, extensive studies have been conducted to understand the mechanism of the resistance of *D. radiodurans* to oxidative stresses, most of which mainly focused on gene regulation, protein functions, and sRNA regulations (38, 39, 46, 50–52). Our previous work has revealed that ionizing radiation can cause a significantly increased 8-oxoG-RNA concentration in *D. radiodurans* (39). However, the contribution of molecular systems that affect the processing of RNA modifications in the context of oxidative stress resistance of *D. radiodurans* is limited. Here, we further showed that *D. radiodurans* possess several RBPs (particularly PNPase and RhlB) that can preferably bind and affect the cellular availability of the 8-oxoG-modified RNA to protect cells under oxidative stress; this represents another mechanism underlying the extreme resistance of *D. radiodurans* to oxidative stresses.

8-oxoG modification in RNA can cause a decrease in the fidelity of gene expression or translation and is closely related to a range of diseases (5, 14, 20). Based on previous studies, 8-oxoG-modified RNA can be recognized by RBPs and further processed via pathways related to RNA decay or programmed cell death (8, 15, 17, 22, 23). Several proteins that exhibit selective binding to RNA molecules containing 8-oxoG have been uncovered, such as Auf1, PCBP1, PCBP2, and PNPase (24, 25, 29). However, most of these proteins have been characterized in model organisms (*E. coli* and HeLa cells).

In the present study, we discovered a set of RBPs (PNPase, RhlB, RpsA, and Rho) that selectively bind 8-oxoG-modified RNA in the nonmodel bacterium *D. radiodurans*. Given that only PNPase was previously shown to exhibit preferential binding to 8-oxoG-modified RNA (28, 29), these data indicate that RhlB, RpsA, and Rho in *D. radiodurans* may also have similar functions. However, unfortunately, we were not able to confirm the importance of RpsA and Rho in controlling RNA oxidation since deletion of these proteins could not be achieved, likely due to their critical roles for cell viability in *D. radiodurans*. Importantly, through EMSA analysis, we determined that PNPase and RhlB showed much higher binding affinities to 8-oxoG-modified RNA than RpsA and Rho (Table 1), implying that PNPase and RhlB may play prominent roles in combating RNA oxidation in *D. radiodurans*. Therefore, we only focused on PNPase and RhlB in this study. Interestingly, PNPase and RhlB bind to 8-oxoG-modified RNA in a dose-independent manner, which was not observed for other 8-oxoG binding proteins (e.g., Auf1 in HeLa cells showed dose-dependent binding on 8-oxoG-modified oligonucleotides) (26). It is possible that the binding pocket of PNPase and RhlB can be saturated by a single 8-oxoG, which prevents the further binding of additional 8-oxoG bases. However, the underlying mechanism requires further investigation.

The preferential binding of PNPase and RhlB to 8-oxoG-modified RNA relative to unmodified RNA suggests their important roles in 8-oxoG-RNA processing and oxidative stress response in *D. radiodurans*. Indeed, deletion of PNPase and RhlB resulted in reduced survivability of *D. radiodurans* and elevated 8-oxoG-RNA levels upon H_2O_2 exposure (Fig. 4A and Fig. 5A). On the contrary, there is no change of 8-oxoG-DNA when the expression of the two proteins was abolished (Fig. 5B), suggesting that the reduced viability of the Δ*pnp* and Δ*rhlB* mutant strains under H_2O_2 may only be related to the accumulation of oxidized RNA in the cells (not oxidized DNA). Notably, the expression of PNPase and RhlB were observed to significantly decrease at both mRNA and protein levels under H_2O_2 stress (Fig. 4B to D); a similar phenomenon has been observed with human 8-oxoG recognizing RBPs (53). The decreased expression of PNPase and RhlB

under H$_2$O$_2$ stress might be beneficial to other functional roles of these proteins, such as sRNA regulations and RNA decay (54–56). It is also worth noting that the impact of PNPase and RhlB seems more significant under high level of oxidative stress (Fig. 4A and Fig. 5A; see also Fig. S4C). In contrast, their effect under normal physiological conditions is little (Fig. 4A and Fig. 5A; see also Fig. S4C), when antioxidant proteins (i.e., catalase) are sufficient to combat the adverse effects caused by the lower (basal) level of oxidative stress.

Importantly, it is known that the degradation activity of PNPase can be impaired by secondary structures (e.g., stem-loop structures) occurring internally or at the 3′ end of the RNA substrates (57). Combining proteomics and biochemical approaches, we identified that PNPase associates with RhlB in *D. radiodurans* independent of RNA (Fig. 6D). Further, both PNPase and RhlB are important for preventing the accumulation of 8-oxoG-modified RNA and for the survival of *D. radiodurans* under oxidative stress (Fig. 4 and 5), and the double-deletion experiments of the two proteins indicate that they may function cooperatively to eliminate the 8-oxoG-modified RNA (Fig. 7A and B). In addition, RhlB facilitates PNPase's degradation on dsRNA *in vitro* (Fig. 7C). Based on these results, we speculate that RhlB may selectively capture structured RNAs that are modified with 8-oxoG and break down the secondary structures to enable PNPase's functions in *D. radiodurans*. Unfortunately, we were not able to confirm this hypothesis since no dsRNA can be observed using 8-oxoG-modified oligonucleotides since 8-oxoG interferes with the base-pairing and potentially affects the dsRNA formation (14, 49). Moreover, despite the fact that PNPase has been demonstrated to preferably bind 8-oxoG-modified RNA in numerous organisms (28, 29), in this study we cannot distinguish whether PNPase/RhlB modulates the cellular availability of 8-oxoG-modified RNAs by direct and/or indirect degradation or by sequestration. We also cannot exclude the possibility that PNPase and RhlB exhibit redundant roles or act at different levels in modulating RNA oxidation. The investigation into these topics will need to be performed in future work.

Lastly, our study reveals the interactions of PNPase with many other proteins in *D. radiodurans*, including DNA repair proteins, and RNA polymerase subunits (Fig. 6A; see also Table S2). Although some of the proteins identified from the PNPase-coIP experiment may result from indirect protein-protein interactions, it is very likely that PNPase participates in a large protein network in *D. radiodurans*, cooperatively functioning with other proteins in multiple pathways. Interestingly, RpsA (the ribosomal protein S1) was also found to interact with PNPase in *D. radiodurans* in an RNA-independent fashion (Fig. 6D), suggesting that PNPase may also interact with RpsA to form a complex to cope with the oxidized RNA. Among many of the PNPase-involved protein complexes, the RNA degradosome is the most famous; it shows wide compositional variation across different bacteria (33). Thus far, the composition and function of the degradosome in *D. radiodurans* are still unknown. In our coIP data, we found that RhlB and RNase J (DR_2417/Rnj) can also be copurified with PNPase in *D. radiodurans* (Fig. 6A; see also Table S2), indicating that RNase J or RhlB may function as part of the *D. radiodurans* degradosome together with PNPase.

Altogether, our work provides new insights into how *D. radiodurans* scavenges oxidized RNA molecules under oxidative stress and significantly expands our knowledge of how RBPs recognize and eliminate oxidized RNA in bacteria. In our future studies, we also hope to explore the location of the 8-oxoG modifications in the transcriptome of *D. radiodurans* and analyze how the modification locations contribute to the detoxification of RNA oxidation.

MATERIALS AND METHODS

Strains and culture conditions. The *D. radiodurans* strain R1 (ATCC 13939) and its derivatives were cultured aerobically in TGY media (1% tryptone, 0.1% glucose, 0.5% yeast extract) at 32°C or on agar plates when required. *E. coli* DH10b and BL21(DE3) strains were grown aerobically in Luria-Bertani (LB) media (10 g/L tryptone, 10 g/L NaCl, and 5 g/L yeast extract) or plates at 37°C. All strains used in this study are listed in Table S3. When necessary, antibiotics were used at the following concentrations:

ampicillin at 100 μg/mL for *E. coli*, chloramphenicol at 15 μg/mL for *E. coli* and 3.4 μg/mL for *D. radiodurans*, and kanamycin at 50 μg/mL for *E. coli* and 16 μg/mL for *D. radiodurans*.

Construction of plasmids and strains. The *D. radiodurans* mutants were constructed by double crossover recombination of a kanamycin resistance cassette into the genome to replace the intended mutation region as described previously (46). Gene tagging with 3×FLAG was achieved by replacing the stop codon with a 3×FLAG coding sequence using the same strategy. To construct the *D. radiodurans* strains expressing C-terminal His$_6$-tagged PNPase and RhlB, the coding sequences were amplified and cloned into the SacII- and BamHI-cut sites after *groES* promoter on the pRADgro plasmid (50). The reverse primers contain CACCACCACCACCACCAC at the 5′ end to replace the stop codon. The strain expressing His$_6$ was constructed by inserting CACCACCACCACCACCAC between the same cut sites on the pRADgro plasmid using Gibson assembly. The recombinant plasmids were transformed into *D. radiodurans* strains, and the resulting colonies were selected on TGY plates with chloramphenicol. For the construction of plasmids expressing His-tagged proteins, the coding region of each protein was amplified and cloned into the NdeI- and BamHI-cut sites on pET28a plasmid so that the His$_6$ tag can be added to the N-terminal ends of the proteins for purification. The resultant plasmids were then electrotransformed into the *E. coli* BL21(DE3) strains. The colonies were then confirmed by PCR screening and Sanger sequencing. All plasmids and primers used in this study are listed in Table S3 and S4, respectively.

RNA affinity chromatography. To identify specific 8-oxoG binding proteins, a 24-mer RNA oligonucleotide (8-oxoG ×1; 5′-biotin-NNNGNNNNNGNNNNN8-oxoGNNNNNGNN-3′; N stands for a random base [A/T/C/G]) was chemically synthesized for the RNA affinity chromatography assay, and an unmodified oligonucleotide (Ctrl; 5′-biotin-NNNGNNNNNGNNNNNGNNNNNGNN-3′) was used as a control. To determine whether the binding of PNPase and RhlB is dose dependent, three more RNA oligonucleotides containing different numbers of 8-oxoG were used: 8-oxoG ×2 (5′-biotin-NNNGNNNNNGNNNNN8-oxoGNNNNN8-oxoGNN-3′), 8-oxoG ×3 (5′-biotin-NNNGNNNNN8oxoGNNNNN8-oxoGNNNNN8-oxoGNN-3′), and 8-oxoG×4 (5′-biotin-NNN8oxoGNNNNN8oxoGNNNNN8-oxoGNNNNN8-oxoGNN-3′). Next, 100 mL of *D. radiodurans* cells (in biological triplicates) was harvested at an optical density at 600 nm (OD$_{600}$) of 0.8, washed, and resuspended in lysis buffer (1 mM Tris-HCl [pH 8.0] containing 1 mM phenylmethylsulfonyl fluoride [PMSF]). The cells were then lysed using sonication as described before (46). Next, the cell extracts were collected by centrifugation at 12,000 × *g* to obtain whole-cell lysates from the supernatant, and the concentrations were measured by using the Bradford assay (Bio-Rad). Then, 500 μg of the lysates or purified His$_6$-tagged proteins were precleared with 500 μg of Dynabead MyOne Streptavidin C1 (Thermo Fisher Scientific) in 300 μL of binding buffer (10 mM Tris-Cl [pH 7.5], 150 mM KCl, 1.5 mM MgCl$_2$, 0.05% [vol/vol] IGEPAL CA-630) for 30 min at 4℃ with rotation in the presence of 0.4 U/mL SUPERase-In RNase Inhibitor (Thermo Fisher Scientific) and 125 μg of yeast tRNA (Sigma-Aldrich). Then, 10 μg of biotinylated modified/unmodified RNA baits in 20 mM Tris-Cl (pH 7.5) was refolded by heating at 90℃ for 10 min, followed by incubation with precleared lysates or His$_6$-tagged protein (200 μg) for 30 min at room temperature and then for 2 h at 4℃. The mixture was then added to 500 μg of Dynabeads MyOne Streptavidin C1 preblocked with BSA (1%) and tRNA (50 μg/mL) for 2 h at 4℃. The RNA-protein complexes were pulled down and washed with 900 μL of wash buffer (10 mM Tris-Cl [pH 7.5], 100 mM NaCl, 150 mM KCl, 1.5 mM MgCl$_2$, 0.05% [vol/vol] IGEPAL CA-630) three times. The bead pellets were then eluted using 20 μL of high-salt elution buffer (10 mM Tris-Cl [pH 7.5], 500 mM NaCl, 150 mM KCl, 1.5 mM MgCl$_2$, 0.05% [vol/vol] IGEPAL CA-630). To increase the yield, the elution step was repeated, and the eluates were combined. The eluted proteins were then analyzed by SDS-PAGE, Western blotting, or LC-MS/MS.

Electrophoretic mobility shift assays. N-terminal His$_6$ tagged proteins were purified from the soluble lysate using Ni-NTA agarose (Qiagen) as described previously (58). EMSAs were performed to determine the binding affinity of the proteins to 8-oxoG-modified and unmodified RNA *in vitro*, as described previously (59). The oligonucleotides used in the affinity chromatography assays (same compositions except with no biotin on the 5′ end) were radiolabeled with 10 μCi of [γ-^{32}P]ATP (Perkin-Elmer) by T4 polynucleotide kinase (New England BioLabs) and purified using an Oligo Clean & Concentrator kit (Zymo Research). Next, 10 fmol of radiolabeled RNA probes (at a final concentration of 1 nM) was incubated with increasing amounts of each purified proteins (0 to 10,000 nM, final concentration) in 10 μL reactions in 1× binding buffer (20 mM Tris-HCl [pH 8.0], 1 mM MgCl$_2$, 20 mM KCl, 10 mM Na2HPO4-NaH$_2$PO$_4$ [pH 8.0], and 10% glycerol containing 500 nM heparin as a nonspecific competitor). When testing PNPase, final protein concentrations of approximately 0 to 1,000 nM were used, and the incubation was performed in TMK buffer (50 mM Tris-HCl [pH 7.5], 50 mM KCl, 10 mM [CH$_3$COO]$_2$Mg, 10% glycerol, 500 nM heparin). Reaction mixtures were incubated at 37℃ for 1 h and then resolved by native electrophoresis in 0.5× Tris-borate-EDTA running buffer at 4℃ for 3 h at 120 V using 5% polyacrylamide native gels. The gels were dried onto 3MM Whatman paper, exposed to a phosphor screen, and visualized using a Typhoon FLA 700 (GE Health Life Science). The signals were analyzed, and the equilibrium dissociation constant (K_d) was determined as described earlier (60). Each EMSA was performed at least two times.

Coimmunopurification of PNPase and RhlB. pRADgro plasmids carrying His$_6$ or His$_6$-tagged PNPase and RhlB were transformed into the *D. radiodurans* R1 wild-type strain or *D. radiodurans* strains carrying 3×FLAG chromosomally tagged RhlB, RpsA, or Rho proteins. These strains (in biological triplicates) were grown to an OD$_{600}$ of 0.8 and treated with formaldehyde (1% [wt/vol]) at room temperature for 15 min with continuous shaking to facilitate the cross-linking. Glycine was then added to a final concentration of 0.125 M to quench the cross-linking reaction. Cross-linked cells (50 mL) were washed three times with ice-cold binding buffer (20 mM Na$_3$PO$_4$, 300 mM NaCl, 10 mM imidazole, 1 mM MgCl$_2$, and 20 mM KCl [pH 7.4] with 1 mM PMSF). Cells were then resuspended and lysed by sonication as described

above. After lysis, the crude extracts were centrifuged at 12,000 rpm for 10 min at 4°C to collect the supernatant. For each His$_6$-tag pulldown reaction, 1 mL of cell extracts containing 500 μg of protein was incubated with 50 μL of Ni-NTA magnetic beads (New England BioLabs) for 30 min at room temperature. The protein-protein mixtures were then washed using 500 μL of wash buffer (20 mM Na$_3$PO$_4$, 300 mM NaCl, and 20 mM imidazole [pH 7.4] with 1 mM PMSF) three times and eluted using 20 μL of elution buffer (20 mM Na$_3$PO$_4$, 300 mM NaCl, and 500 mM imidazole [pH 7.4] with 1 mM PMSF). To increase the yield, the elution step was repeated, and the eluates were combined. The protein samples were then concentrated by dialysis and subjected to LC-MS/MS or Western blotting. To determine whether the protein interactions are RNA-dependent, one set of samples was incubated with 2 μg of RNase A and 5 U of RNase T$_1$ (Thermo Fisher Scientific) for 15 min at 22°C after cell lysis. coIP samples from cell lysates treated with or without RNase were subjected to Western blotting as described below.

LC-MS/MS. Proteins obtained from RNA affinity chromatography or coIP were resuspended in SDS sample buffer (0.5 M Tris-HCl [pH 6.8], 25% [vol/vol] glycerol, 0.5% [wt/vol] SDS, 0.5% [wt/vol] bromophenol blue, 0.05% [vol/vol] β-mercaptoethanol). The mixtures were denatured at 95°C for 5 min before being run ~3 mm into the 12% Mini-Protean TGX precast protein gels (Bio-Rad). After staining with Coomassie Bright Blue (Sigma-Aldrich), the protein bands were excised using a clean razor blade. The gel tubes were then dehydrated with 100% acetonitrile (Sigma-Aldrich), reduced with 10 mM dithiothreitol (DTT) for 30 min at room temperature, followed by alkylation with 50 mM iodoacetamide in the dark for another 30 min. The gels were washed, rehydrated, and then digested with 10 ng/μL trypsin (Thermo Fisher Scientific) overnight at 37°C. Proteins were then extracted from the gels using 5% formic acid and 1:2 (vol/vol) 5% formic acid-acetonitrile. The samples were sent for LC-MS/MS analysis at the University of Texas ICMB proteomics facility. The resulting protein spectral counts were searched against the UniProt *D. radiodurans* R1 (ATCC 13939) database using Sequest HT in Proteome Discoverer 1.4 and normalized to the total ion intensity. The identifications were validated with Scaffold v4.4.1 (Proteome Software) with >99.0% probability and with a minimum of two peptides at 99.0% peptide probability. The false discovery rate was set at 1% for peptides and 5% for protein identification. The difference between two strains or fractions was calculated by using a Student *t* test, and the *P* values were adjusted by the Benjamini-Hochberg method (61).

Western Blotting. Protein samples were resuspended in the SDS sample buffer, boiled at 95°C for 10 min, separated by 12% Mini-Protean TGX precast protein gels (Bio-Rad), and transferred to nitrocellulose membranes (Bio-Rad) using a Trans-Blot semidry transfer cell (Bio-Rad). Membranes were blocked with 5% milk powder overnight at 4°C and incubated for 1 h with monoclonal Anti-Flag M2-peroxidase antibody (Sigma-Aldrich, 1:1,000 dilution) or His$_6$ tag monoclonal antibody (Thermo Fisher Scientific, 1:2,000 dilution) at room temperature. Afterward, the membranes were further incubated with antimouse IgG(H+L)/HRP conjugate (Promega) for another 1 h. After three washes with TBST, chemiluminescence was detected by using Clarity Western enhanced chemiluminescence substrate (Bio-Rad). Protein samples were visualized by Coomassie staining in parallel to show the equivalent protein loading in each lane. Quantitation of Western blot band intensities was done using the CLIQS software (TotalLab). Each Western blot analysis was performed at least three times.

Measurement of cell survival. *D. radiodurans* strains (WT, Δpnp, $\Delta rhlB$, and Δpnp $\Delta rhlB$) were grown to an OD$_{600}$ of 0.8 and stressed with different dosages (0 to 200 mM) of H$_2$O$_2$ (Sigma-Aldrich) for 30 min at 4°C in the dark. The cells were serially diluted (10^{-3} to 10^{-5}) with sterilized 1× phosphate-buffered saline and plated on TGY agar plates with appropriate antibiotics. The plates were incubated at 32°C for 3 days, and the colonies were counted. The relative survival was calculated as the percentage of the number of colonies under each H$_2$O$_2$ concentration compared to that for no H$_2$O$_2$ treatment.

Determination of 8-oxoG-RNA and 8-oxoG-DNA levels. *D. radiodurans* strains (WT, Δpnp, $\Delta rhlB$, and Δpnp $\Delta rhlB$) were grown to an OD$_{600}$ of 0.8, stressed by 100 mM H$_2$O$_2$ (Sigma-Aldrich) for 30 min at 4°C in the dark, and then collected by centrifugation at 12,000 × *g* for 5 min. Total RNA was extracted and purified using the Direct-zol RNA miniprep kit (Zymo Research) according to the manufacturer's protocol. DNA contamination in the RNA samples was removed by DNase digestion during the extraction. Total DNA was extracted using a Wizard genomic DNA purification kit (Promega), including an RNase digestion step to remove the RNA contamination in the samples. The levels of 8-oxoG in DNA and RNA samples were measured by a competitive ELISA (using a DNA/RNA oxidative damage EIA kit from Cayman Chemical) as described previously (62). Briefly, 1 μg of DNA or RNA from each sample was digested to nucleosides by nuclease P1 (Sigma-Aldrich) in 20 mM sodium acetate for 2 h at 37°C and dephosphorylated using the calf intestinal alkaline phosphatase (New England BioLabs) in a 100 mM Tris buffer (JT Baker) for 1 h at 37°C. Then, 1 μg of digested DNA or RNA samples was incubated with 8-oxoG antibody and tracers for 16 h. After extensive washes, the absorbance values were measured using a wavelength of 412 nm in the BioTek Cytation3 plate reader, and the results were analyzed as recommended by the manufacturer. All solutions used in this assay were nitrogen purged to ensure that no extra oxidation is introduced in the experiments.

Determination of H$_2$O$_2$ content in *D. radiodurans* cell cultures. *D. radiodurans* strains (WT, Δpnp, $\Delta rhlB$, and $\Delta katA$) were grown to an OD$_{600}$ of 0.8 and stressed by 0 or 100 mM H$_2$O$_2$ (Sigma-Aldrich) for 30 min at 4°C in the dark. The H$_2$O$_2$ level in the cultures was immediately determined using an Amplex Red kit (Thermo Fisher Scientific) as recommended by the manufacturer.

Growth curve measurement. Growth curves of *D. radiodurans* strains were evaluated using a Plate Reader (BioTek). Biological triplicates of each strain were distributed into 96-well plates with 200 μL TGY media. The initial OD$_{600}$ was adjusted to 0.1, and the turbidity (600 nm) was measured every 30 min for 8 h as the cultures grew with shaking at 32°C. Catalase (Sigma-Aldrich) was added to a final concentration of 50 or 100 nM when needed.

RNA helicase and degradation activity assay. The combinational effect of PNPase and RhlB on structured RNA *in vitro* was performed as described previously (36). A 22-mer RNA oligonucleotide (5′-ACAGUAUUU<u>GGUACUGCGCUCU</u>-3′) was radiolabeled at the 5′ end using 10 μCi of [γ-^{32}P]ATP (Perkin-Elmer) and T4 polynucleotide kinase (New England BioLabs). To generate dsRNA, the labeled 22-mer RNA oligonucleotide was incubated with an unlabeled 11-mer RNA oligonucleotide (5′-<u>AGAGCGCA GUACC</u>-3′, with complementary base pairs with the 22-mer oligonucleotide [underlined]) in RNA annealing buffer (10 mM Tris-HCl [pH 8.0], 20 mM KCl) by heating to 95°C for 5 min, followed by slow cooling ($\gg$1 h) to room temperature. To maximize the hybridization efficiency, the 22-mer RNA oligonucleotide and the 11-mer RNA oligonucleotide were incubated at a ratio of 1:1.5 (mol/mol). 10 nM (final concentration) of double-stranded RNA duplex or 22-mer single-stranded RNA was incubated with PNPase (100 nM, final concentration) or RhlB (150 nM, final concentration) alone or with mixtures of PNPase and RhlB at 32°C for 30 min in 10 μL of activity buffer (20 mM Tris-HCl [pH 7.5], 5 mM MgCl$_2$, 0.1 mM DTT, 5% glycerol, 10 mM K$_2$HPO$_4$, 50 mM KCl, and 3 mM ATP). The reaction was then stopped by adding 10 μL of 2$\times$ RNA loading buffer (New England BioLabs). The samples were separated on a 20% polyacrylamide native gel and visualized using Typhoon FLA 700 (GE Health Life Science).

RT-qPCR. RT-qPCR was performed using a Luna Universal One-Step RT-qPCR kit (New England Biolabs, Inc.) on a ViiA7 instrument (Applied Biosciences). cDNA was synthesized using 50 ng of RNA at 55°C for 10 min, followed by denaturation at 95°C for 1 min and 40 cycles of 95°C for 10 s and 60°C for 30 s. 16S rRNA was used as the internal normalization control. The relative expression of each gene was calculated using the $2^{-\Delta\Delta CT}$ method (63). The experiments were performed in biological triplicate. The primers used for RT-qPCR are listed in Table S4.

Statistics analysis. Student two-sided t-tests were used to assess the significance of the results. Values of $P \leq$ 0.05, 0.01, or 0.001 were considered to be statistically significant (*), highly significant (**), or extremely significant (***), respectively, as indicated by asterisks in the figures.

Data availability. The LC-MS/MS raw data have been deposited in the ProteomeXchange Consortium via the PRIDE partner repository (64) under the data set identifiers PXD028861 (RNA affinity chromatography) and PXD028866 (PNPase- and RhlB-coIP).

SUPPLEMENTAL MATERIAL

Supplemental material is available online only.
SUPPLEMENTAL FILE 1, PDF file, 3.2 MB.
SUPPLEMENTAL FILE 2, XLSX file, 0.02 MB.
SUPPLEMENTAL FILE 3, XLSX file, 0.02 MB.
SUPPLEMENTAL FILE 4, XLSX file, 0.01 MB.
SUPPLEMENTAL FILE 5, XLSX file, 0.01 MB.

ACKNOWLEDGMENTS

REFERENCES

1. Imlay JA. 2003. Pathways of oxidative damage. Annu Rev Microbiol 57:395–418. https://doi.org/10.1146/annurev.micro.57.030502.090938.
2. Fridovich I. 1978. The biology of oxygen radicals. Science 201:875–880. https://doi.org/10.1126/science.210504.
3. Santanam N, Ramachandran S, Parthasarathy S. 1998. Oxygen radicals, antioxidants, and lipid peroxidation. Semin Reprod Endocrinol 15:275–280.
4. Sekiguchi M, Tsuzuki T. 2002. Oxidative nucleotide damage: consequences and prevention. Oncogene 21:8895–8904. https://doi.org/10.1038/sj.onc.1206023.
5. Li Z, Chen X, Liu Z, Ye W, Li L, Qian L, Ding H, Li P, Aung LHH. 2020. Recent advances: molecular mechanism of RNA oxidation and its role in various diseases. Front Mol Biosci 7:184. https://doi.org/10.3389/fmolb.2020.00184.
6. Salim S. 2014. Oxidative stress and psychological disorders. Curr Neuropharmacol 12:140–147. https://doi.org/10.2174/1570159X11666131120230309.
7. Nunomura A, Perry G, Aliev G, Hirai K, Takeda A, Balraj EK, Jones PK, Ghanbari H, Wataya T, Shimohama S, Chiba S, Atwood CS, Petersen RB, Smith MA. 2001. Oxidative damage is the earliest event in Alzheimer disease. J Neuropathol Exp Neurol 60:759–767. https://doi.org/10.1093/jnen/60.8.759.
8. Nunomura A, Lee HG, Zhu X, Perry G. 2017. Consequences of RNA oxidation on protein synthesis rate and fidelity: implications for the pathophysiology of neuropsychiatric disorders. Biochem Soc Trans 45:1053–1066. https://doi.org/10.1042/BST20160433.
9. Evans MD, Dizdaroglu M, Cooke MS. 2004. Oxidative DNA damage and disease: induction, repair and significance. Mutat Res 567:1–61. https://doi.org/10.1016/j.mrrev.2003.11.001.
10. Liu M, Gong X, Alluri RK, Wu J, Sablo T, Li Z. 2012. Characterization of RNA damage under oxidative stress in Escherichia coli. Biol Chem 393:123–132. https://doi.org/10.1515/hsz-2011-0247.

11. Ishibashi T, Hayakawa H, Ito R, Miyazawa M, Yamagata Y, Sekiguchi M. 2005. Mammalian enzymes for preventing transcriptional errors caused by oxidative damage. Nucleic Acids Res 33:3779–3784. https://doi.org/10.1093/nar/gki682.

12. Tanaka M, Chock PB, Stadtman ER. 2007. Oxidized messenger RNA induces translation errors. Proc Natl Acad Sci U S A 104:66–71. https://doi.org/10.1073/pnas.0609737104.

13. Simms CL, Hudson BH, Mosior JW, Rangwala AS, Zaher HS. 2014. An active role for the ribosome in determining the fate of oxidized mRNA. Cell Rep 9:1256–1264. https://doi.org/10.1016/j.celrep.2014.10.042.

14. Wang JX, Gao J, Ding SL, Wang K, Jiao JQ, Wang Y, Sun T, Zhou LY, Long B, Zhang XJ, Li Q, Liu JP, Feng C, Liu J, Gong Y, Zhou Z, Li PF. 2015. Oxidative modification of miR-184 enables it to target Bcl-xL and Bcl-w. Mol Cell 59:50–61. https://doi.org/10.1016/j.molcel.2015.05.003.

15. Ishii T, Sekiguchi M. 2019. Two ways of escaping from oxidative RNA damage: selective degradation and cell death. DNA Repair (Amst) 81:102666. https://doi.org/10.1016/j.dnarep.2019.102666.

16. Malfatti MC, Antoniali G, Codrich M, Tell G. 2021. Coping with RNA damage with a focus on APE1, a BER enzyme at the crossroad between DNA damage repair and RNA processing/decay. DNA Repair (Amst) 104:103133. https://doi.org/10.1016/j.dnarep.2021.103133.

17. Yan LL, Zaher HS. 2019. How do cells cope with RNA damage and its consequences? J Biol Chem 294:15158–15171. https://doi.org/10.1074/jbc.REV119.006513.

18. Kraszewska E, Drabinska J. 2020. Nudix proteins affecting microbial pathogenesis. Microbiology (Reading) 166:1110–1114. https://doi.org/10.1099/mic.0.000993.

19. Taddei F, Hayakawa H, Bouton MF, Cirinesi AM, Matic I, Sekiguchi M, Radman M. 1997. Counteraction by MutT protein of transcriptional errors caused by oxidative damage. Science 278:128–130. https://doi.org/10.1126/science.278.5335.128.

20. Tanaka M, Chock PB. 2021. Oxidative modifications of RNA and its potential roles in biosystem. Front Mol Biosci 8:685331. https://doi.org/10.3389/fmolb.2021.685331.

21. Radak Z, Boldogh I. 2010. 8-Oxo-7,8-dihydroguanine: links to gene expression, aging, and defense against oxidative stress. Free Radic Biol Med 49:587–596. https://doi.org/10.1016/j.freeradbiomed.2010.05.008.

22. Li Z, Malla S, Shin B, Li JM. 2014. Battle against RNA oxidation: molecular mechanisms for reducing oxidized RNA to protect cells. Wiley Interdiscip Rev RNA 5:335–446. https://doi.org/10.1002/wrna.1214.

23. Simms CL, Zaher HS. 2016. Quality control of chemically damaged RNA. Cell Mol Life Sci 73:3639–3653. https://doi.org/10.1007/s00018-016-2261-7.

24. Ishii T, Hayakawa H, Sekiguchi T, Adachi N, Sekiguchi M. 2015. Role of Auf1 in elimination of oxidatively damaged messenger RNA in human cells. Free Radic Biol Med 79:109–116. https://doi.org/10.1016/j.freeradbiomed.2014.11.018.

25. Ishii T, Igawa T, Hayakawa H, Fujita T, Sekiguchi M, Nakabeppu Y. 2020. PCBP1 and PCBP2 both bind heavily oxidized RNA but cause opposing outcomes, suppressing or increasing apoptosis under oxidative conditions. J Biol Chem 295:12247–12261. https://doi.org/10.1074/jbc.RA119.011870.

26. Ishii T, Hayakawa H, Igawa T, Sekiguchi T, Sekiguchi M. 2018. Specific binding of PCBP1 to heavily oxidized RNA to induce cell death. Proc Natl Acad Sci U S A 115:6715–6720. https://doi.org/10.1073/pnas.1806912115.

27. Wu J, Jiang Z, Liu M, Gong X, Wu S, Burns CM, Li Z. 2009. Polynucleotide phosphorylase protects Escherichia coli against oxidative stress. Biochemistry 48:2012–2020. https://doi.org/10.1021/bi801752p.

28. Hayakawa H, Sekiguchi M. 2006. Human polynucleotide phosphorylase protein in response to oxidative stress. Biochemistry 45:6749–6755. https://doi.org/10.1021/bi052585l.

29. Hayakawa H, Kuwano M, Sekiguchi M. 2001. Specific binding of 8-oxoguanine-containing RNA to polynucleotide phosphorylase protein. Biochemistry 40:9977–9982. https://doi.org/10.1021/bi010595q.

30. Gonzalez-Rivera JC, Orr AA, Engels SM, Jakubowski JM, Sherman MW, O'Connor KN, Matteson T, Woodcock BC, Contreras LM, Tamamis P. 2020. Computational evolution of an RNA-binding protein towards enhanced oxidized-RNA binding. Comput Struct Biotechnol J 18:137–152. https://doi.org/10.1016/j.csbj.2019.12.003.

31. Wu J, Li Z. 2008. Human polynucleotide phosphorylase reduces oxidative RNA damage and protects HeLa cell against oxidative stress. Biochem Biophys Res Commun 372:288–292. https://doi.org/10.1016/j.bbrc.2008.05.058.

32. Cameron TA, Matz LM, De Lay NR. 2018. Polynucleotide phosphorylase: not merely an RNase but a pivotal post-transcriptional regulator. PLoS Genet 14:e1007654. https://doi.org/10.1371/journal.pgen.1007654.

33. Tejada-Arranz A, de Crécy-Lagard V, de Reuse H. 2020. Bacterial RNA degradosomes: molecular machines under tight control. Trends Biochem Sci 45:42–57. https://doi.org/10.1016/j.tibs.2019.10.002.

34. Płociński P, Maclos M, Houghton J, Niemiec E, Płocińska R, Brzostek A, Słomka M, Dziadek J, Young D, Dziembowski A. 2019. Proteomic and transcriptomic experiments reveal an essential role of RNA degradosome complexes in shaping the transcriptome of Mycobacterium tuberculosis. Nucleic Acids Res 47:5892–5905. https://doi.org/10.1093/nar/gkz251.

35. Mackie GA. 2013. RNase E: at the interface of bacterial RNA processing and decay. Nat Rev Microbiol 11:45–57. https://doi.org/10.1038/nrmicro2930.

36. Liou GG, Chang HY, Lin CS, Lin-Chao S. 2002. Dead box RhlB RNA helicase physically associates with exoribonuclease PNPase to degrade double-stranded RNA independent of the degradosome-assembling region of RNase E. J Biol Chem 277:41157–41162. https://doi.org/10.1074/jbc.M206618200.

37. Lin P-H, Lin-Chao S. 2005. RhlB helicase rather than enolase is the β-subunit of the Escherichia coli polynucleotide phosphorylase (PNPase)–exoribonucleolytic complex. Proc Natl Acad Sci U S A 102:16590–16595. https://doi.org/10.1073/pnas.0500994102.

38. Lim S, Jung JH, Blanchard L, De Groot A. 2019. Conservation and diversity of radiation and oxidative stress resistance mechanisms in Deinococcus species. FEMS Microbiol Rev 43:19–52. https://doi.org/10.1093/femsre/fuy037.

39. Tsai CH, Liao R, Chou B, Contreras LM. 2015. Transcriptional analysis of Deinococcus radiodurans reveals novel small RNAs that are differentially expressed under ionizing radiation. Appl Environ Microbiol 81:1754–1764. https://doi.org/10.1128/AEM.03709-14.

40. Chen X, Wurtmann EJ, Van Batavia J, Zybailov B, Washburn MP, Wolin SL. 2007. An ortholog of the Ro autoantigen functions in 23S rRNA maturation in D. radiodurans. Genes Dev 21:1328–1339. https://doi.org/10.1101/gad.1548207.

41. Joe MH, Jung SW, Im SH, Lim SY, Song HP, Kwon O, Kim DH. 2011. Genome-wide response of Deinococcus radiodurans on cadmium toxicity. J Microbiol Biotechnol 21:438–447. https://doi.org/10.4014/jmb.1012.12021.

42. Szklarczyk D, Morris JH, Cook H, Kuhn M, Wyder S, Simonovic M, Santos A, Doncheva NT, Roth A, Bork P, Jensen LJ, von Mering C. 2017. The STRING database in 2017: quality-controlled protein–protein association networks, made broadly accessible. Nucleic Acids Res 45:D362–D368. https://doi.org/10.1093/nar/gkw937.

43. Nicastro G, Taylor IA, Ramos A. 2015. KH–RNA interactions: back in the groove. Curr Opin Struct Biol 30:63–70. https://doi.org/10.1016/j.sbi.2015.01.002.

44. Young CL, Karbstein K. 2011. The roles of S1 RNA-binding domains in Rrp5's interactions with pre-rRNA. RNA 17:512–521. https://doi.org/10.1261/rna.2458811.

45. Sinha D, Zheng JJ, Tsui HCT, Richardson JD, de Lay NR, Winkler ME. 2020. S1 domain RNA-binding protein CvfD is a new posttranscriptional regulator that mediates cold sensitivity, phosphate transport, and virulence in Streptococcus pneumoniae D39. J Bacteriol 202:e00245-20. https://doi.org/10.1128/JB.00245-20.

46. Han R, Fang J, Jiang J, Gaidamakova EK, Tkavc R, Daly MJ, Contreras LM. 2020. Signal recognition particle RNA contributes to oxidative stress response in Deinococcus radiodurans by modulating catalase localization. Front Microbiol 11:613571. https://doi.org/10.3389/fmicb.2020.613571.

47. Feng Y, Huang H, Liao J, Cohen SN. 2001. Escherichia coli poly(A)-binding proteins that interact with components of degradosomes or impede RNA decay mediated by polynucleotide phosphorylase and RNase E. J Biol Chem 276:31651–31656. https://doi.org/10.1074/jbc.M102855200.

48. Rojano-Nisimura AM, Haning K, Janovsky J, Vasquez KA, Thompson JP, Contreras LM. 2020. Codon selection affects recruitment of ribosome-associating factors during translation. ACS Synth Biol 9:329–342. https://doi.org/10.1021/acssynbio.9b00344.

49. Shibutani S, Takeshita M, Grollman AP. 1991. Insertion of specific bases during DNA synthesis past the oxidation-damaged base 8-oxodG. Nature 349:431–434. https://doi.org/10.1038/349431a0.

50. Villa JK, Amador P, Janovsky J, Bhuyan A, Saldanha R, Lamkin TJ, Contreras LM. 2017. A genome-wide search for ionizing-radiation-responsive elements in Deinococcus radiodurans reveals a regulatory role for the DNA gyrase subunit A gene's 5′ untranslated region in the radiation and desiccation response. Appl Environ Microbiol 83:1–19. https://doi.org/10.1128/AEM.00039-17.

51. Chen A, Hernandez-Vargas J, Han R, Cortazar-Martínez O, Gonzalez N, Patel S, Keitz BK, Luna-Barcenas G, Contreras LM. 2021. Small RNAs as a new platform for tuning the biosynthesis of silver nanoparticles for enhanced material and functional properties. ACS Appl Mater Interfaces 13:36769–36783. https://doi.org/10.1021/acsami.1c07400.

52. Villa JK, Han R, Tsai C-H, Chen A, Sweet P, Franco G, Vaezian R, Tkavc R, Daly MJ, Contreras LM. 2021. A small RNA regulates pprM, a modulator of

pleiotropic proteins promoting DNA repair, in *Deinococcus radiodurans* under ionizing radiation. Sci Rep 11:1–14. https://doi.org/10.1038/s41598-021-91335-8.

53. Hayakawa H, Fujikane A, Ito R, Matsumoto M, Nakayama KI, Sekiguchi M. 2010. Human proteins that specifically bind to 8-oxoguanine-containing RNA and their responses to oxidative stress. Biochem Biophys Res Commun 403:220–224. https://doi.org/10.1016/j.bbrc.2010.11.011.

54. De Lay N, Gottesman S. 2011. Role of polynucleotide phosphorylase in sRNA function in *Escherichia coli*. RNA 17:1172–1189. https://doi.org/10.1261/rna.2531211.

55. Ikeda Y, Yagi M, Morita T, Aiba H. 2011. Hfq binding at RhlB-recognition region of RNase E is crucial for the rapid degradation of target mRNAs mediated by sRNAs in *Escherichia coli*. Mol Microbiol 79:419–432. https://doi.org/10.1111/j.1365-2958.2010.07454.x.

56. Tseng YT, Chiou NT, Gogiraju R, Lin-Chao S. 2015. The protein interaction of RNA helicase B (RhlB) and polynucleotide phosphorylase (PNPase) contributes to the homeostatic control of cysteine in *Escherichia coli*. J Biol Chem 290:29953–29963. https://doi.org/10.1074/jbc.M115.691881.

57. Dar D, Sorek R. 2018. High-resolution RNA 3-ends mapping of bacterial Rho-dependent transcripts. Nucleic Acids Res 46:6797–6805. https://doi.org/10.1093/nar/gky274.

58. Liu Y, Han R, Wang J, Yang P, Wang F, Yang B. 2020. Magnesium sensing regulates intestinal colonization of enterohemorrhagic *Escherichia coli* O157:H7. mBio 11:e02470-20. https://doi.org/10.1128/mBio.02470-20.

59. Han R, Haning K, Gonzalez-Rivera JC, Yang Y, Li R, Cho SH, Huang J, Simonsen BA, Yang S, Contreras LM. 2020. Multiple small RNAs interact to coregulate ethanol tolerance in *Zymomonas mobilis*. Front Bioeng Biotechnol 8:1559.

60. Ryder SP, Recht MI, Williamson JR. 2008. Quantitative analysis of protein-RNA interactions by gel mobility shift. Methods Mol Biol 488:99–115. https://doi.org/10.1007/978-1-60327-475-3_7.

61. Li A, Barber RF. 2019. Multiple testing with the structure-adaptive Benjamini–Hochberg algorithm. J R Stat Soc B 81:45–74. https://doi.org/10.1111/rssb.12298.

62. Gonzalez-Rivera JC, Baldridge KC, Wang DS, Patel K, Chuvalo-Abraham JCL, Hildebrandt Ruiz L, Contreras LM. 2020. Posttranscriptional air pollution oxidation to the cholesterol biosynthesis pathway promotes pulmonary stress phenotypes. Commun Biol 3:392. https://doi.org/10.1038/s42003-020-01118-6.

63. Livak KJ, Schmittgen TD. 2001. Analysis of relative gene expression data using real-time quantitative PCR and the 2^{CT} method. Methods 25:402–408. https://doi.org/10.1006/meth.2001.1262.

64. Perez-Riverol Y, Csordas A, Bai J, Bernal-Llinares M, Hewapathirana S, Kundu DJ, Inuganti A, Griss J, Mayer G, Eisenacher M, Pérez E, Uszkoreit J, Pfeuffer J, Sachsenberg T, Yılmaz Ş, Tiwary S, Cox J, Audain E, Walzer M, Jarnuczak AF, Ternent T, Brazma A, Vizcaíno JA. 2019. The PRIDE database and related tools and resources in 2019: improving support for quantification data. Nucleic Acids Res 47:D442–D450. https://doi.org/10.1093/nar/gky1106.